Lattice effects on an impurity center: $CuX_4(NH_3)_2^{2-}$ centers ($X=Cl, Br$) in NH_4X

J. A. Aramburu and M. Moreno
Departamento de Ciencias de la Tierra y Física de la Materia Condensada, Facultad de Ciencias, Universidad de Cantabria, 39005 Santander, Spain
(Received 12 November 1996)

The optical properties of $CuX_4(NH_3)_2^{2-}$ centers embedded in NH_4X lattices ($X=Cl, Br$) where Cu^{2+} occupies an *interstitial* position have been explored through MS $X\alpha$ calculations performed at different values of the Cu^{2+}-X^- (R_{eq}) and Cu^{2+}-N (R_{ax}) distances. The calculations include the effect of the electrostatic potential due to the *rest of the lattice*, V_R, upon the *localized* electrons of the center. It has been shown that V_R decreases significantly the separation between $n_Lp(X)$ and $2p(N)$ orbitals ($n_L=3$ for Cl; $n_L=4$ for Br) and thus plays a key role for understanding the existence of four charge transfer (CT) bands in the optical domain. The high splitting found between orbitals mainly built from $|2p_z(N)\rangle$ and $|2p_j(N)\rangle$ ($j=x,y$) is shown to arise from an *internal* splitting in the NH_3 molecule *transferred* to the complex. From the R_{eq} and R_{ax} dependence of CT transitions, it is shown that the 600-cm^{-1} redshift undergone by the first CT transition of $CuCl_4(NH_3)_2^{2-}$ in NH_4Cl just below $T_c=243$ K involves an R_{eq} *increase* of ~ 2 pm in agreement with Raman data. The present results stress the importance of V_R for a right understanding of properties due to impurities placed at *off-center* positions. [S0163-1829(97)07225-1]

I. INTRODUCTION

Optical and electron paramagnetic resonance (EPR) data due to impurities in insulators have usually been explained considering *only* the complex formed by the impurity and the anions of different species adjacent to the impurity. This idea was reinforced by the theoretical work carried out by Sugano and Shulman.[1] These authors pointed out that in cubic lattices like $KMgF_3$ the electrostatic potential due to the *rest of the lattice* (called V_R) upon the electrons of a MF_6 complex ($M=Ni^{2+}$, Mn^{2+}, etc.) formed by a *substitutional* divalent impurity is certainly very flat. Therefore, if the electrons responsible for the properties of the impurity are localized *in* the complex, the potential V_R influences neither the optical transitions nor the wave functions and can be ignored.

Subsequent work on substitutional impurities in cubic materials has revealed the validity of such an idea. For instance, it has been shown experimentally that a given complex embedded in different host lattices, but of the *same type*, does not exhibit the same EPR and optical parameters through the series.[2–8] This fact has reasonably been explained simply through the changes on the metal-ligand distance of the complex, R, induced by changing from one host lattice another one.[3–5,6,8] Owing to this fact, a parameter like $10Dq$ has been used to measure the actual R value of impurities like Mn^{2+} or Ni^{2+} in fluoroperovskites.[6,8,4]

It can reasonably be expected that the degree of flatness contained in V_R depends, however, not only on the *type* of lattice where the impurity is placed, but also on the *position* (substitutional, interstitial, off center) occupied by the impurity in the host lattice. The importance of this idea was partially realized in the analysis[9] of the experimental $10Dq$ values of CrF_3 and K_2NaCrF_6. Both materials[9] involve the same CrF_6^{3-} unit, but possess a *different* space group. Experimentally, it has been found that in the first compound $R=1.90$ Å and $10Dq=14\,650$ cm^{-1}, while, in K_2NaCrF_6, $R=1.93$ Å and $10Dq=16\,100$ cm^{-1}. These results can hardly be understood in terms of isolated CrF_6^{3-} complexes subjected to a constant electrostatic potential. In fact, experimental studies on impurities like Mn^{2+} or Cr^{3+} in high-symmetry sites have shown[6,8,10–12] that the R dependence of $10Dq$ can be written as

$$10Dq = KR^{-n}, \tag{1}$$

where the exponent n is close to 5. Theoretical calculations[13,14] on isolated complexes are in agreement with that experimental result, while the microscopic origin of Eq. (1) within a molecular orbital scheme has been analyzed recently.[15] The amazing increase of $10Dq$ on passing from CrF_3 ($R=1.90$ Å) to K_2NaCrF_6 ($R=1.93$ Å) has reasonably been explained through the different form of V_R in both lattices.[9] In CrF_3, V_R induces an *additional* separation between $3d$ and ligand orbitals favoring a diminution of $10Dq$. A similar situation to this one has recently been encountered when comparing[16] the EPR data due to Ag^{2+} placed in a perovskite lattice ($CsCdF_3$) and NaF. In the latter case, it has been shown that V_R induces a supplementary decrement of $g_\parallel - g_0$.

It can be expected that effects arising from the nonflatness of V_R will be *more pronounced* for optical transitions involving *jumps* from a mainly *ligand level* to a mainly d level. This work is devoted to show the relevance of V_R for understanding the experimental charge transfer (CT) spectra of $Cu(NH_3)_2X_4^{2-}$ centers formed in NH_4X ($X=Cl, Br$) lattices.[17–21] Such centers are good candidates for observing effects coming from the electrostatic potential of the rest of the lattice because Cu is placed in an *interstitial* position and *not* in a substitutional one (Fig. 1). Owing to this fact, the X^- and NH_3 ligands are placed in *nonequivalent* crystallographic directions of the NH_4X lattice. Moreover, the N-Cu^{2+} (R_{ax}) and Cl-Cu^{2+} (R_{eq}) distances are very different, favoring different V_R values at Cl^- or NH_3 positions.

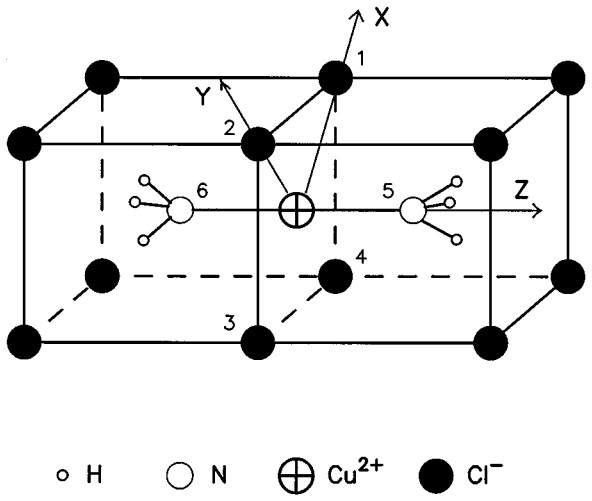

FIG. 1. Picture of the $CuX_4(NH_3)_2^{2-}$ center formed in NH_4X (X=Cl, Br) host lattices. Cu^{2+} is placed interstitially in the middle of a (100) face made of X^- ions, while two NH_3 molecules occupy NH_4^+ vacancies.

Although R_{ax} and R_{eq} are not known for the present cases in compounds like $Cu(NH_3)_2X_2$ (X=Cl, Br), the $Cu(NH_3)_2X_4^{2-}$ complexes are formed and so R_{ax} and R_{eq} have been measured[22,23] through x-ray diffraction. For instance, for the bromine complex,[22] R_{ax}=2.03 Å and R_{eq} =2.87 Å have been measured. These distances coincide with those expected for the $CuBr_4(NH_3)_2^{2-}$ complex placed in the undistorted NH_4Br lattice as shown in Fig. 1. A similar situation occurs for the $CuCl_4(NH_3)_2^{2-}$ complex for which the metal-ligand distances will be close to R_{ax} =1.96 Å and R_{eq}=2.76 Å.

The study of $CuX_4(NH_3)_2^{2-}$ centers is also attractive because of their peculiar electronic structure. In fact, in tetragonal centers of d^9 ions (Cu^{2+}, Ag^{2+}, Ni^+) the unpaired electron usually lies in a $\sim x^2-y^2$ orbital, while in the present cases it is located in a $\sim 3z^2-r^2$ orbital, giving rise to σ bonding with *both* equatorial and axial ligands. On the other hand, a $|3z^2-r^2\rangle$ orbital can be hybridized with the $|4s\rangle$ orbital of the central ion in a D_{4h} symmetry. It has been pointed out that such an hybridization is very sensitive to changes of R_{eq} and R_{ax}, inducing remarkable changes of the isotropic hyperfine constant A_{iso}, well observed experimentally.[24,25]

The CT spectra of systems containing CuX_6^{4-} (X =Cl, Br) units is composed[26–28] of *two* prominent bands related to jumps from the *two* mainly ligand e_u orbitals. By contrast, in the CT spectra[29] of $CuBr_4(NH_3)_2^{2-}$ in NH_4Br at T=14 K (in the cubic phase of NH_4Br) it can clearly be seen the existence of four bands (Fig. 2) peaked at 25 500, 28 500, 31 600, and 37 500 cm^{-1}. In the case of $CuCl_4(NH_3)^{2-}$, apart from two dominant bands peaked at 33 700 and 39 500 cm^{-1}, another band peaked at 43 200 cm^{-1} is also visible.[30] If we accept that the two lowest bands in Fig. 2 involve $Br^-\rightarrow Cu^{2+}$ jumps, it is not certainly easy to assign the bands peaked at 31 600 and 37 300 cm^{-1} as being due to $NH_3\rightarrow Cu^{2+}$ jumps. In fact, following the optical electronegativity of Br (χ=2.8) and NH_3 (χ=3.3), one could expect that the $NH_3\rightarrow Cu^{2+}$ CT bands of $CuBr_4(NH_3)_2^{2-}$ *start* at about 45 000 cm^{-1}.

A reasonable explanation of these experimental features is attempted through this work by means of MS $X\alpha$ calculations. Particular attention is paid to the *form* of V_R inside the $CuX_4(NH_3)_2^{2-}$ centers as well as to its influence upon the observed CT spectrum of such Cu^{2+} centers.

II. THEORETICAL

Properly speaking, the symmetry group displayed by a $CuX_4(NH_3)_2^{2-}$ unit is not D_{4h}, but C_{2h}. We have verified, however, that in the orbitals of interest in the present work, the splitting induced by hydrogen atoms is essentially negligible. Therefore we shall label the electron orbitals according to the D_{4h} group. A picture of relevant one-electron levels is offered in Fig. 3. We have assumed for the NH_3 molecule the

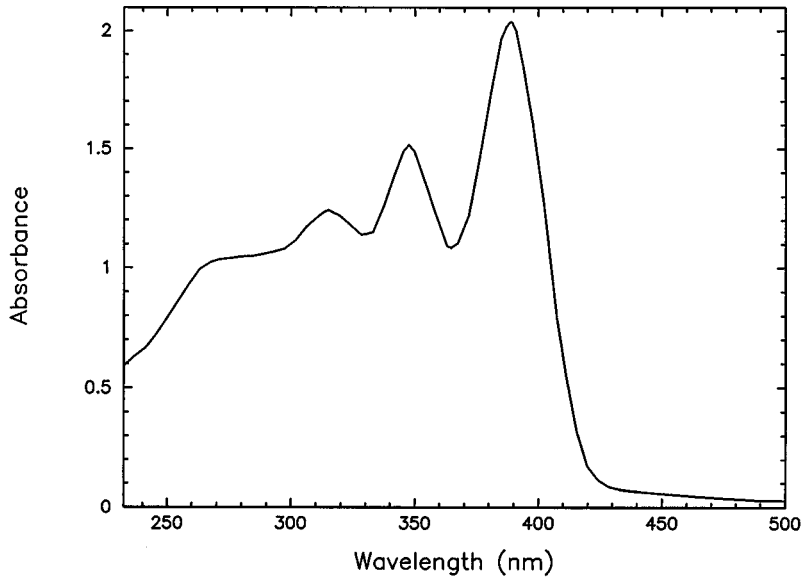

FIG. 2. Charge transfer spectrum of the $CuBr_4(NH_3)_2^{2-}$ center in NH_4Br taken at 14 K (Ref. 29).

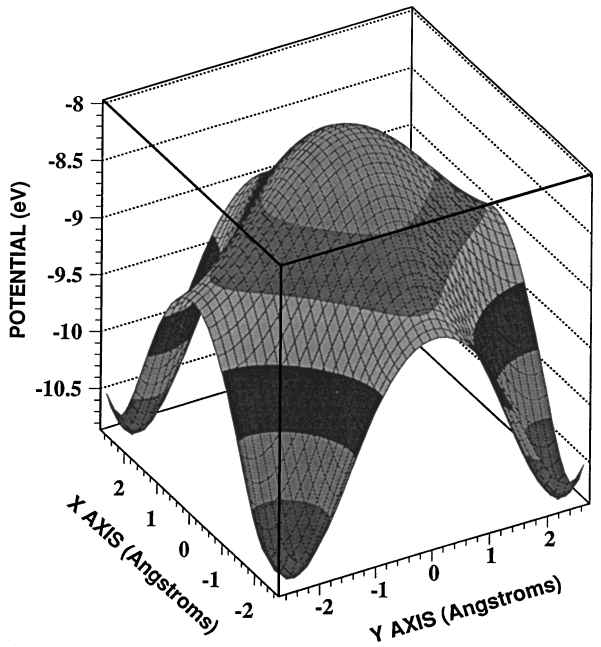

FIG. 3. Picture of the potential energy $U_R(\mathbf{r})$ (in eV) due to the rest of the NH_4Cl lattice on an electron of the $CuCl_4(NH_3)_2^{2-}$ center taken in the xy plane of Fig. 1. The point $x=0$, $y=0$ corresponds to Cu^{2+} while the four Cl^- ions are found at $(x=\pm 2.7,\ y=0)$; $(x=0,\ y=\pm 2.7)$. All distances are given in Å. In this region the lowest value of U_R is reached at the Cu^{2+} position, while, at Cl^-, U_R is 1 eV higher.

same experimental geometry as the free molecule, while R_{ax} and R_{eq} distances have been varied, keeping a compressed D_{4h} geometry. This follows the interest in exploring the sensitivity of crystal-field (CF) and CT transition energies to changes of R_{ax} and R_{eq} as well as to the lack of precise R_{ax} and R_{eq} values for the equilibrium positions of the present systems.

For a Cu^{2+} impurity placed in a local D_{4h} symmetry, electric dipole CT jumps of the type $|L\rangle \rightarrow |a_{1g}^*\rangle$ require that $|L\rangle$ belong to E_u or A_{2u}. For a $CuX_4(NH_3)_2^{2-}$ center, it is easy to see that *three* E_u levels and *two* A_{2u} levels should appear, considering the four n_Lp atomic orbitals of halogens ($n_L=3$ for Cl, $n_L=4$ for Br) and the two $2p$(N) orbitals. The electronic structure of E_u and A_{2u} levels involved in the allowed CT transitions is rather complex. So in a A_{2u} level there is in principle a *hybridization* between equatorial ligand orbitals and axial ligand orbitals as well as an admixture of the $|4p_i(\mathrm{Cu})\rangle$ wave function. Besides for a E_u orbital, there are also *two* different types of linear combination of atomic orbitals (LCAO) involving *only* the equatorial ligands. The inclusion of the six involved H atoms lowers the symmetry to C_{2h}, giving rise to a splitting of all e_u orbitals. In our calculations such a splitting is found to be *always less* than 30 cm^{-1}. It is worth noting, however, that the $1s$ orbitals of six H atoms play an important role in the description of some relevant charge transfer levels. This point is discussed in detail in Sec. III. Calculations on $CuX_4(NH_3)_2^{2-}$ centers embedded in NH_4X lattices have been performed by means of the self-consistent field multiple-scattering $X\alpha$ (MS $X\alpha$) method.[31,32] Atomic sphere radii were chosen using the Norman criterion,[33] with a small modification in order to take into account the specificity of the H atoms.[34] So sphere radii that contain the atomic number of electrons were calculated from the initial molecular potential derived from neutral atoms. Then these radii were reduced by a factor of 0.98, given an average overlap ratio of about 20%. Always using this procedure, not only the experimental CF and CT transitions of several centers involving d^9 and d^3 ions have been reasonably explained, but also their sensibility to variations of metal-ligand distances.[16,35,36] In $CuX_4(NH_3)_2^{2-}$ complexes, the calculated H radii are, however, greater than N-H distances, and so we have always considered radii equal to 1 bohr.[34] The α values used in the atomic regions were those determined by Schwarz.[37] Transition energies were considered using the Slater transition-state procedure.[31] More details can be found in Ref. 35.

In order to clarify the role played by the rest of the lattice potential, V_R, upon the electronic properties of $CuX_4(NH_3)_2^{2-}$ centers, two types of calculations have been carried out for each couple of R_{eq} and R_{ax} distances. In the first one, V_R has simply been approximated by a constant potential using a Watson sphere of $+2e$ charge coincident with the outer sphere. In the second type, V_R on an atomic sphere has been taken as the Madelung potential due to all X^- and NH_4^+ ions of the lattice *not* involved in the $CuX_4(NH_3)_2^{2-}$ center. In this case, a weighted average potential has been used for the intersphere region, while a Q/r $(Q=+2e)$ potential has been taken for the outer sphere. Ewald's method[38] has been used for computing V_R.

III. REMAINDER OF THE LATTICE POTENTIAL

Let us take the origin of coordinates in Fig. 1 at the Cu^{2+} position. The electrostatic potential at a point $\mathbf{r}$ of the $CuX_4(NH_3)_2^{2-}$ center due to the rest of the lattice can easily be calculated as

$$V_R(\mathbf{r}) = V_T(\mathbf{r}) - V_C(\mathbf{r}). \tag{2}$$

Here $V_T(\mathbf{r})$ means the electrostatic potential due to the full NH_4X lattice at $\mathbf{r}$, while $V_C(\mathbf{r})$ is the potential generated by the four X^- anions at $(\pm a\sqrt{2}/2,0,0)$ and $(0,\pm a\sqrt{2}/2,0)$ and the two NH_4^+ ions at $(0,0\pm \frac{1}{2}a)$ in the perfect lattice.

For the present purposes, when $\mathbf{r}$ corresponds to a lattice point R_L, the self-potentials $V_T(\mathbf{r})$ and $V_C(\mathbf{r})$ should be employed instead of $V_T(\mathbf{r})$ and $V_C(\mathbf{r})$. It just means that the contribution arising from the ion at $\mathbf{R}_L$ should be omitted.[38] The potential energy for an electron ''feeling'' V_R is just $U_R=(-e)V_R$ and is shown in Figs. 3 and 4. Both figures clearly reveal that U_R is far from being flat in the $CuX_4(NH_3)_2^{2-}$ center placed in NH_4Cl. For instance, U_R at the Cl^- position is about 1 eV smaller than at the Cu^{2+} position. At the same time, U_R increases the energy of electrons at the NH_3 position with respect to those at the Cu^{2+} position by 2.8 eV.

The main aspects about U_R depicted in Figs. 3 and 4 can easily be derived using the results for the potential $\psi(\mathbf{r})$ of the so-called neutralized cubic lattice explained in Ref. 38. For instance, at the Cu^{2+} position V_T is simply given by

$$V_T(\mathrm{Cu}^{2+}) = e\{\psi(1/2,0,0) - \psi(1/2,1/2,0)\}, \tag{3}$$

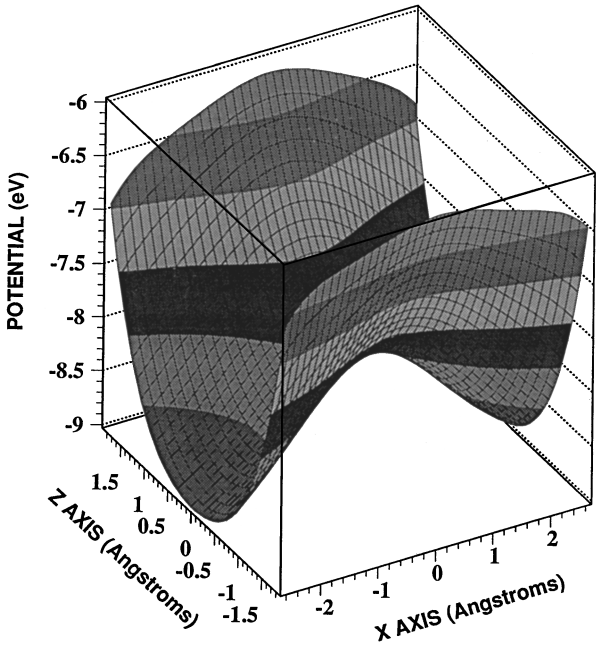

FIG. 4. Picture of $U_R(\mathbf{r})$ for the electrons of the $CuCl_4(NH_3)_2^{2-}$ center embedded in NH_4Cl when $\mathbf{r}$ varies along the xz plane of Fig. 1. The difference between the potential energy at N($x=0$, $z=1.9$) and at Cl ($x=2.7$, $z=0$) is equal to 4.8 eV. The distances are given in Å.

where $\psi(1/2,0,0)=-0.096/a$, $\psi(1/2,1/2,0)=-0.583/a$, and a is the lattice parameter of the CsCl-like lattice. From here and Eq. (2), it is derived that

$$U_R(\mathrm{Cu}^{2+})=-2.14\,\frac{e^2}{a} \tag{4}$$

and, similarly,

$$U_R(X^-)=-2.43\,\frac{e^2}{a},\quad U_R(\mathrm{NH_3})=-1.58\,\frac{e^2}{a}. \tag{5}$$

As the difference found between $U_R(\mathrm{NH_3})$ and $U_R(X^-)$ is certainly high (about 4 eV), one can thus envisage that U_R plays a relevant role for achieving a right microscopic understanding of optical transitions due to $CuX_4(NH_3)_2^{2-}$ centers in NH_4X lattices.

IV. RESULTS

The transition energies for the allowed CT and the parity-forbidden CF transitions of the $CuBr_4(NH_3)_2^{2-}$ center in NH_4Br calculated at different R_{ax} and R_{eq} values are displayed in Table I. The results obtained either including the properly V_R or taking it just as a constant are both reported in Table I. Insight into the composition of the one-electron orbitals associated with the $^2A_{1g}$ ground state is given in Table II. In this case the figures correspond to a calculation performed at $R_{ax}=2.0$ Å, $R_{eq}=2.85$ Å, and including the effect of the rest of the lattice electrostatic potential V_R.

The ordering of relevant one-electron orbitals found in the present calculations is outlined in Table I. For the three couples of axial and equatorial distances, the unpaired electron is found to be placed in the antibonding $5a_{1g}$ level. Though this level is mainly built from the $3z^2-r^2$ wave function of Cu (Table II), it exhibits, however, a significant admixture of $4p$(Br), $2p$(N), and also $4s$(Cu) wave functions. That admixture reflects, but indirectly, the presence of bonding levels mainly built from $4p$(Br) and $2p$(N) not far from the antibonding CF levels. This is confirmed by Table I where the separation between the highest CF excitation and the lowest allowed CT transition is always less than 13 000 cm^{-1}.

The lowest CT transitions involve the $4e_u$, $3e_u$, and $3a_{2u}$ levels. It is worth noting that $4e_u$ and $3e_u$ levels exhibit an almost pure $4p$(Br) character, while in $3a_u$, though mainly built from $4p$(Br), the amount of $2p$(N) character increases by a factor close to 7 with respect to what is found in $3e_u$. The highest allowed CT transition involves a $2e_u$ orbital where only a 1% of $4p$(Br) is present. Nevertheless, this $2e_u$ orbital is far from displaying a pure $2p$(N) character because it involves about 30% of $1s$ orbitals of six hydrogens.

As shown in Table I, the inclusion of V_R in the calculations gives rise to *substantial* changes in the CT spectrum.

TABLE I. Values of crystal-field and allowed charge transfer transitions of the $CuBr_4(NH_3)_2^{2-}$ unit embedded in NH_4Br calculated for different values of the axial (R_{ax}) and equatorial (R_{eq}) metal-ligand distances given in pm. In the calculation called ''Madelung,'' the effect of the rest of the lattice potential V_R has been considered, while in the so-called Watson V_R has been approximated by a constant potential. The energy of transitions (given in cm^{-1}) have been computed using the Slater's transition-state method. Experimental values are included for comparison (Ref. 29).

		$R_{eq}=285$	$R_{ax}=190$	$R_{eq}=285$	$R_{ax}=200$	$R_{eq}=280$	$R_{ax}=200$
Transition	Experimental	Madelung	Watson	Madelung	Watson	Madelung	Watson
$3b_{1g}\rightarrow 5a_{1g}$	—	9600	7980	8050	6210	8080	6290
$3e_g\rightarrow 5a_{1g}$	~13300	15650	14500	14430	12850	15030	13940
$2b_{2g}\rightarrow 5a_{1g}$	~13300	16290	14950	14870	13360	15450	13930
$4e_u\rightarrow 5a_{1g}$	25550	28950	23890	26950	22220	27920	23100
$3a_{2u}\rightarrow 5a_{1g}$	28530	31110	26720	28300	24690	29080	25660
$3e_u\rightarrow 5a_{1g}$	31600	33300	28300	31460	26800	32830	28070
$2a_{2u}\rightarrow 5a_{1g}$	36790	43730	51630	37170	45390	38130	45320
$2e_u\rightarrow 5a_{1g}$		73790	85090	69430	80420	70180	80610

TABLE II. Charge distribution (in %) corresponding to relevant one-electron levels of $CuX_4(NH_3)_2^{2-}$ centers embedded in NH_4X lattices. The values given here come from calculations properly including the effect of the rest of the lattice potential. First-row results correspond to $X=$Br computed at $R_{eq}=285$ pm, $R_{ax}=200$ pm, while those given in the second row are for $X=$Cl calculated at $R_{eq}=270$ pm, $R_{ax}=190$ pm.

	Cu			X		N		H
Orbital	$3d$	$4s$	$4p$	n_Ls	n_Lp	$2s$	$2p$	$1s$
$5a_{1g}$	57.34	6.15		1.62	20.58	1.51	12.15	0.65
	60.56	8.98		2.49	15.98	1.14	10.27	0.55
$4e_u$			1.11	0.21	98.33		0.22	0.13
			0.87	0.14	98.50		0.33	0.16
$3e_u$			2.49	0.20	95.49		1.22	0.60
			2.02	0.11	95.51		1.57	0.79
$3a_{2u}$			1.30		90.43	1.16	6.69	0.42
			3.17		82.33	1.44	12.22	0.83
$2a_{2u}$			18.95		8.86	2.11	64.89	5.18
			18.92		15.50	1.61	59.05	4.91
$2e_u$			0.90	0.42	1.36		67.15	30.17
			1.15	0.45	1.90		66.43	30.07

Let us call $\Delta_{1,5}$ the separation between the lowest ($4e_u \rightarrow 5a_{1g}$) and the highest ($2e_u \rightarrow 5a_{1g}$) allowed CT excitations. When V_R is taken as constant $\Delta_{1,5} = 57\,000$ cm^{-1}, while when it is properly included $\Delta_{1,5}$ becomes equal only to 42 000 cm^{-1}. The origin of this significant reduction can basically be understood from the results given in Sec. III. It was shown there that V_R tends to raise the one-electron energies of $2p$(N) orbitals while decreasing the corresponding to $4p$(Br) orbitals.

As shown in Table I, the agreement between the experimental[29] CT transitions and the calculated ones is certainly improved when the effect of V_R is properly taken into account. For instance, at $R_{ax}=2.00$ Å and $R_{eq}=2.85$ Å the present calculations not only predict the existence of four (and not five) CT transitions of the $CuBr_4(NH_3)_2^{2-}$ center in NH_4Br lying in the optical domain, but also the reported values are in reasonable agreement with experimental[29] data. By contrast, when the effect of the actual V_R is discarded the separation $\Delta_{1,4}$ between the lowest and highest CT transitions lying in the optical domain is about 20 000 cm^{-1}, while experimentally $\Delta_{1,4}$ is close to 11 000 cm^{-1}.

The calculated $3b_{1g} \rightarrow 5a_{1g}$ and $3e_g \rightarrow 5a_{1g}$ CF transitions are also close to the experimental figures. As expected, these transitions coming from the $d \rightarrow d$ transitions of copper are less sensitive to the inclusion of V_R.

Let us mention that the analysis of experimental data[29] indicated that the second CT transition observed at 14 K corresponds to $3e_u \rightarrow 5a_{1g}$ and not to $3a_{2u} \rightarrow 5a_{1g}$ as obtained in the present calculations. The separation between such transitions amounts, however, only to ~ 3000 cm^{-1} and is only resolved at low temperatures in the cubic phase of NH_4Br.

The results[30] for the $CuCl_4(NH_3)_2^{2-}$ center in NH_4Cl collected in Table III display similar trends to those corresponding for the $CuBr_4(NH_3)_2^{2-}$ center in NH_4Br. Nevertheless, though the ordering of levels is the same, the first $4e_u \rightarrow 5a_{1g}$ CT transition is calculated to appear at about 36 000 cm^{-1} for $R_{eq}=2.70$ Å and $R_{ax}=1.90$ Å, implying a blueshift of ~ 9000 cm^{-1} with respect to what was found for $CuBr_4(NH_3)_2^{2-}$. This blueshift is thus consistent with the higher optical electronegativity[31] of chlorine ($\chi=3.0$) when compared to that of bromine ($\chi=2.8$).

TABLE III. Transition energies (in cm^{-1}) of the $CuCl_4(NH_3)_2^{2-}$ center embedded in NH_4Cl computed at different values of the metal-ligand distances R_{ax} and R_{eq} (given in pm). In the calculations denoted as ''Madelung,'' the effect of V_R has been included. Experimental values (measured at 14 K) are included for comparison purposes (Ref. 30).

		$R_{eq}=260$	$R_{ax}=190$	$R_{eq}=270$	$R_{ax}=190$	$R_{eq}=270$	$R_{ax}=200$
Transition	Experimental	Madelung	Watson	Madelung	Watson	Madelung	Watson
$3b_{1g} \rightarrow 5a_{1g}$	9300	10730	8960	10590	8820	9180	6920
$3e_g \rightarrow 5a_{1g}$	12400	17030	16260	16020	14950	15250	13600
$2b_{2g} \rightarrow 5a_{1g}$	13950	17570	16530	16610	15010	15440	13670
$4e_u \rightarrow 5a_{1g}$	33720	38280	30620	36150	29440	33990	26350
$3a_{2u} \rightarrow 5a_{1g}$		37170	32830	37500	31650	33940	28250
$3e_u \rightarrow 5a_{1g}$	39480	42850	35450	40070	33520	37980	30650
$2a_{2u} \rightarrow 5a_{1g}$	43200	45250	52190	44250	52050	37630	45850
$2e_u \rightarrow 5a_{1g}$		75700	85960	75500	85670	71310	

The increase of CT excitation energies on going from $CuBr_4(NH_3)_2^{2-}$ to $CuCl_4(NH_3)_2^{2-}$ also favors a parallel decrement of covalency well observed in Table III. For instance, for the $5a_{1g}$ orbital of $CuCl_4(NH_3)_2^{2-}$ the fraction of $3p$(Cl) character is 16%, while in the case of $CuBr_4(NH_3)_2^{2-}$ the fraction of $4p$(Br) amounts to 21% (Table III).

As regards the theoretical values of CT excitation energies in $CuCl_4(NH_3)_2^{-2}$, only those obtained considering the true V_R potential lead again to a reasonable agreement with experimental findings. In particular, the present calculations support the fact that the shoulder observed experimentally[30] at 43 200 cm^{-1} can be reasonably assigned to a $2a_{2u} \rightarrow 5a_{1g}$ transition. Also, the first assignment of the experimental transitions at 33 720 and 39 480 cm^{-1} as being due to electron jumps from the mainly $3p$(Cl) e_u orbitals is supported by the present theoretical study. With respect to the $3a_{2u} \rightarrow 5a_{1g}$ transition, the present results indicate that it would lie between the $4e_u \rightarrow 5a_{1g}$ and $3e_u \rightarrow 5a_{1g}$ transitions. Experimentally, such a transition has, however, not yet been resolved maybe because the associated band is masked by those coming from $4e_u \rightarrow 5a_{1g}$ and $3e_u \rightarrow 5a_{1g}$ transitions whose bandwidth is close to 2000 cm^{-1}. The calculated fifth allowed CT transition appears out of the optical domain as also happened for the $CuBr_4(NH_3)_2^{2-}$ center in NH_4Br.

Although the present calculations indicate that only four of the allowed CT transitions lie in the optical range, it is also necessary to *understand why* the difference between the a_{2u} and $2e_u$ orbitals is so high. In fact, taking as a guide the case of $CuCl_4(NH_3)_2^{2-}$ *both* orbitals exhibit a *dominant* $2p$(N) character, but the a_{2u} orbital is separated *by only* 4000 cm^{-1} from the $3e_u$ orbital, which exhibits a strong $3p$(Cl) character. This makes possible a significant presence of $3p$(Cl) character in a_{2u} and also of $2p$(N) character in $3a_{2u}$. By contrast, the $2e_u$ orbital, being mainly built from $2p$(N), is certainly far from the mainly $3p$(Cl) levels. This feature is thus consistent with the almost negligible $2p$(N) character displayed by $3e_u$ and $4e_u$ orbitals.

Let us now analyze the origin of the separation (called $\Delta_{4,5}$) between the $2a_{2u} \rightarrow 5a_{1g}$ and $2e_u \rightarrow 5a_{1g}$ transitions. As shown Tables I and III $\Delta_{4,5}$ is about 32 000 cm^{-1} for the present $CuX_4(NH_3)_2^{2-}$ centers formed in NH_4X lattices. For comparison purposes we have first looked at the results of MS $X\alpha$ calculations[39] reached on the *compressed* D_{4h} $CuCl_6^{4-}$ species where *all* the ligands are single Cl^- ions. For instance, for $R_{ax}=2.20$ Å and $R_{eq}=2.80$ Å it is found[39] that $\Delta_{4,5}=3000\ cm^{-1}$, while $\Delta_{4,5}=5500\ cm^{-1}$, for $R_{ax}=2.10$ Å and $R_{eq}=2.80$ Å. These data clearly indicate that $\Delta_{4,5}$ for the $CuX_4(NH_3)_2^{2-}$ center is roughly *one order of magnitude* larger than for the compressed $CuCl_6^{4-}$ species. The value $\Delta_{4,5}$ found for this case is also comparable to the splitting between e_u and a_{2u} orbitals in the simple case of the square-planar $CuCl_4^{2-}$ unit where only equatorial ligands are present.

From this digression it appears that the $\Delta_{4,5}$ splitting in $CuX_4(NH_3)_2^{2-}$ centers should arise mainly from an *intramolecular* splitting of the ammonia molecule. This idea is certainly reinforced when we look at the electronic structure[40] of NH_3. As this C_{3v} molecule is nearly planar, the highest occupied orbital is a A singlet, being also denoted as 3σ. In this orbital, mainly composed of $|p_z(N)\rangle$, the lone pair of NH_3 is placed. The z direction involved in $|p_z(N)\rangle$ is depicted in Fig. 1. Below the A singlet orbital, a doublet E orbital (also denoted as 1π) appears where bonding effects with the hydrogen atoms are much stronger. This is again a direct consequence of the 78 ° angle between a NH direction and the principal axis of the NH_3 molecule. Associated with this important difference between the bonding in the A singlet and the E doublet, a separation of $\sim 40\,000\ cm^{-1}$ appears between them.[40] This separation can of course be related to the $\Delta_{4,5}$ values found for $CuX_4(NH_3)_2^{2-}$ centers (Tables I and III). Also, it is now easy to understand why the amount of $1s$(H) in $2e_u$ (Table II) is about 6 times higher than the corresponding to the $2a_{2u}$ orbital, which as pointed out is related to the orbital of free NH_3 where the lone pair is located.

Let us now briefly focus on the sensitivity to R_{ax} and R_{eq} changes displayed by the energy E of CT and CF transitions. As shown in Tables I and III the CT transition energies are in general more sensitive than CF transitions like $3e_g \rightarrow 5a_{1g}$ or $2b_g \rightarrow 5a_{1g}$ to variations of metal-ligand distances. This feature has also been found for other d^9 systems as well as for Cr^{3+} in fluorides.[35,36,39] Analyzing the R_i dependence for CT transition energy in transition-metal complexes with moderate covalency, it has been shown[36] that $\partial E/\partial R_i$ mainly reflects $\partial(U_M - U_L)/\partial R_i$. Here U_M means the electrostatic energy experienced by an electron placed in the metallic cation due to charged ligands, while U_L denotes the same contribution when the electron is located on a ligand. As normally $U_M > U_L$ and $\partial U_M/\partial R_i > \partial U_L/\partial R_i$, the negative sign of $\partial E/\partial R_i$ simply reflects an increase of the repulsive U_M energy upon decreasing R_i. For the $4e_u \rightarrow 5a_{1g}$ and $3e_u \rightarrow 5a_{1g}$ transitions of $CuX_4(NH_3)_2^{2-}$ centers, $\partial E/\partial R_{eq}$ would be about $-300\ cm^{-1}$/pm. This figure is smaller than $\partial E/\partial R_{eq} \cong -600\ cm^{-1}$/pm measured[41] and calculated[42] for CT transitions of the square-planar $CuCl_4^{2-}$ unit. This significant difference partially reflects the smaller value of R_{eq} corresponding to $CuCl_4^{2-}$ ($R_{eq}=226$ pm) when compared to the equilibrium R_{eq} value of $CuX_4(NH_3)_2^{2-}$. On passing from $CuCl_4^{2-}$ to CrF_6^{3-}, the increase of ligand number as well as the diminution of R ($R=190$ pm for CrF_6^{3-} typically) leads[36] to values $\partial E/\partial R_{eq} \cong -1500\ cm^{-1}$/pm.

Upon cooling from room temperature, the NH_4Cl lattice experiences a structural phase transition at $T_c=243$ K which *decreases* by 0.4 pm the lattice parameter.[43] The optical spectrum due to the $CuX_4(NH_3)_2^{2-}$ center embedded in NH_4Cl shows,[30] however, that the first $4e_u \rightarrow 5a_{1g}$ transition undergoes a *redshift* of 600 cm^{-1} (instead of a blueshift) just below T_c. This redshift was reasonably explained in terms of an *outwards* relaxation of Cl^- ions just below T_c, an idea which was corroborated by subsequent Raman experiments.[44] Accepting $\partial E/\partial R_{eq} \cong -300\ cm^{-1}$/pm, the 600 cm^{-1} redshift would imply an increase of R_{eq}, ΔR_{eq}, equal to $\Delta R_{eq}=2$ pm, which is now in good agreement with the figure derived from Raman data.[44]

V. FINAL REMARKS

It has been shown in the present work that the optical spectrum of $CuX_4(NH_3)_2^{2-}$ centers embedded in NH_4X can

be understood *only* when the effect of V_R is properly taken into account. V_R raises the $2p$(N) levels with respect to the $n_{\mathrm{L}}p(X)$ levels of the halide, favoring the existence of four CT's in the optical range. The fifth allowed CT transition is predicted to appear around 70 000 cm^{-1} mainly as a result of a high *intramolecular splitting* between A and E levels of NH_3 molecules transferred to the center. It is worth noting that the first exciton band of pure NH_4Br appears[45] at 51 000 cm^{-1}, thus preventing the observation of any impurity absorption beyond that frequency.

As regards the intensities displayed by CT transitions, let us recall that in simple complexes like $CuCl_4^{2-}$ CT transitions involving e_u orbitals are much more intense than the allowed $2b_{2u}\rightarrow 3b_{1g}$ ($\sim x^2-y^2$) transitions, which have not been observed experimentally. Denoting a CT jump simply as $\gamma_L\rightarrow\gamma_M$, it has been shown[41,46] that CT transitions where *both* orbitals involve σ bonding exhibit a much higher oscillator strength than the rest of the transitions. It is worth noting that for $CuX_4(NH_3)_2^{2-}$ centers the *four* observed CT transitions involve jumps where the ligand orbital γ_L and the antibonding $5a_{1g}$ *both* involve σ bonding. In fact, at variance with a $\sim x^2-y^2$ orbital, a $\sim 3z^2-r^2$ orbital can establish σ bonding with *both* axial as well as equatorial ligands.

As a general conclusion, the importance that V_R can play for a right understanding of properties due to impurity centers in partially ionic materials has been stressed through the present work. Such a relevance is increased for centers containing neighbor atoms in nonequivalent crystallographic positions. Further work along this line is now under way.

ACKNOWLEDGMENT

This work has been supported by the CICYT under Project No. PB95-0581

[1] S. Sugano and R. G. Shulman, Phys. Rev. **130**, 517 (1963).
[2] J. J. Rousseau, A. Leblé, and J. C. Fayet, J. Phys. (France) **39**, 1215 (1978).
[3] M. T. Barriuso and M. Moreno, Phys. Rev. B **29**, 3623 (1984).
[4] B. Villacampa, R. Cases, V. M. Orera, and R. Alcalá, J. Phys. Chem. Solids **55**, 263 (1993).
[5] B. Villacampa, R. Alcalá, P. J. Alonso, M. Moreno, M. T. Barriuso, and J. A. Aramburu, Phys. Rev. B **49**, 1039 (1994).
[6] F. Rodriguez and M. Moreno, J. Chem. Phys. **84**, 692 (1986).
[7] W. Knierim, A. Honold, U. Brauch, and U. Dürr, J. Opt. Soc. Am. B **3**, 119 (1986).
[8] M. C. Marco de Lucas, F. Rodriguez, and M. Moreno, Phys. Rev. B **50**, 2760 (1994).
[9] K. Pierloot, E. Van Praet, and L. G. Vanquickenborne, J. Chem. Phys. **96**, 4163 (1992).
[10] J. F. Dolan, L. A. Kappers, and R. H. Bartram, Phys. Rev. B **33**, 7339 (1986).
[11] K. Mayrhofer, K. Hochberger, and W. Gebhardt, J. Phys. C **21**, 4393 (1988).
[12] S. J. Duclos, Y. K. Vohra, and A. L. Ruoff, Phys. Rev. B **41**, 5372 (1990).
[13] V. Luaña, M. Bermejo, M. Flórez, J. M. Recio, and L. Pueyo, J. Chem. Phys. **90**, 6409 (1989).
[14] M. Moreno, M. T. Barriuso, and J. A. Aramburu, J. Phys., Condens. Matter. **4**, 9481 (1992).
[15] M. Moreno, M. T. Barriuso, and J. A. Aramburu, Int. J. Quantum Chem. **52**, 829 (1994).
[16] R. Valiente, J. A. Aramburu, M. T. Barriuso, and M. Moreno, Int. J. Quantum Chem. **52**, 1051 (1994).
[17] S. H. Hagen and N. J. Trappeniers, Physica (Utrecht) **47**, 165 (1970).
[18] F. Boettcher and J. M. Spaeth, Phys. Status Solidi B **61**, 465 (1974).
[19] G. Steffen, U. Kaschuba, M. A. Hitchman, and D. Reinen, Z. Naturforsch. B **47**, 465 (1992).
[20] M. Couzi, M. Moreno, and A. G. Breñosa, Solid State Commun. **91**, 481 (1994).
[21] E. Di Mauro and W. Sano, J. Phys., Condens. Matter. **6**, L81 (1994).
[22] F. Hanic and I. A. Cakajdova, Acta Crystallogr. **11**, 610 (1958).
[23] W. R. Clayton and E. A. Meyers,Cryst. Struct. Commun. **5**, 61 (1976).
[24] A. G. Breñosa, M. Moreno, and J. A. Aramburu, J. Phys., Condens. Matter. **3**, 7743 (1991).
[25] S. H. Hagen and N. J. Trappeniers, Physica (Utrecht) **66**, 166 (1973).
[26] K. Kan'no, S. Mukai, and Y. Nakai, J. Phys. Soc. Jpn. **36**, 1492 (1974).
[27] S. Hirako and R. Onaka, J. Phys. Soc. Jpn. **51**, 1255 (1982).
[28] J. Simonetti and D. S. McClure, J. Chem. Phys. **71**, 793 (1979).
[29] A. G. Breñosa, F. Rodriguez, and M. Moreno, J. Phys. C **21**, L623 (1988).
[30] A. G. Breñosa, M. Moreno, and F. Rodriguez, Solid State Commun. **63**, 543 (1987).
[31] J. C. Slater, *Quantum Theory of Molecules and Solids* (McGraw-Hill, New York, 1974), Vol. 4.
[32] K. H. Johnson, Adv. Quantum Chem. **3**, 151 (1982).
[33] J. G. Norman Jr., Mol. Phys. **31**, 1191 (1976).
[34] D. A. Case, Annu. Rev. Phys. Chem. **33**, 151 (1982).
[35] J. A. Aramburu, M. Moreno, and M. T. Barriuso, J. Phys., Condens. Matter. **4**, 9089 (1992).
[36] J. A. Aramburu, M. T. Barriuso, and M. Moreno, J. Phys., Condens. Matter. **8**, 6901 (1996).
[37] K. Schwarz, Phys. Rev. B **5**, 2466 (1972).
[38] M. P. Tosi, Solid State Phys. **16**, 1 (1964).
[39] J. A. Aramburu and M. Moreno, J. Chim Phys. **86**, 871 (1989).
[40] J. C. Slater, *Quantum Theory of Molecules and Solids* (McGraw-Hill, New York, 1963), Vol. 1.
[41] S. Desjardins, S. W. Penfield, S. L. Cohen, R. L. Musselman, and E. I. Solomon, J. Am. Chem. Soc. **105**, 4590 (1983).
[42] J. A. Aramburu, M. Moreno, and A. Bencini, Chem. Phys. Lett. **140**, 462 (1987).
[43] J. E. Callanan, R. D. Weir, and L. A. K. Staveley, Proc. R. Soc. London, Ser. A **372**, 489 (1980).
[44] A. G. Breñosa, M. Moreno, and F. Rodriguez, Phys. Rev. B **44**, 9859 (1991).
[45] M. Itoh, J. Phys. Soc. Jpn. **58**, 329 (1989).
[46] M. T. Barriuso, J. A. Aramburu, C. Daul, and M. Moreno, Int. J. Quantum Chem. **61**, 563 (1997).